PAGEOPH, Vol. 148, Nos. 3/4 (1996) 0033-4553/96/040591-33$1.50 + 0.20/0

Point Source Radiation in Inhomogeneous Anisotropic Structures

IVAN PŠENČÍK[1] and TELESSON NEVES TELES[2]

Abstract—The ray formulae for the radiation from point sources in unbounded inhomogeneous isotropic as well as anisotropic media consist of two factors. The first one depends fully on the type and orientation of the source and on the parameters of the medium at the source. We call this factor the directivity function. The second factor depends on the parameters of the medium surrounding the source and this factor is the well-known geometrical spreading. The displacement vector and the radiation pattern defined as a modulus of the amplitude of the displacement vector measured on a unit sphere around the source are both proportional to the ratio of the directivity function and the geometrical spreading.

For several reasons it is desirable to separate the two mentioned factors. For example, there are methods in exploration seismics, which separate the effects of the geometrical spreading from the observed wave field (so-called true amplitude concept) and thus require the proposed separation. The separation also has an important impact on computer time savings in modeling seismic wave fields generated by point sources by the ray method. For a given position in a given model, it is sufficient to calculate the geometrical spreading only once. A multitude of various types of point sources with a different orientation can then be calculated at negligible additional cost.

In numerical examples we show the effects of anisotropy on the geometrical spreading, the directivity and the radiation pattern. Ray synthetic seismograms due to a point source positioned in an anisotropic medium are also presented and compared with seismograms for an isotropic medium.

Key words: Inhomogeneous anisotropic media, point sources, the ray Green function, the directivity function, the radiation pattern, ray synthetic seismograms.

1. Introduction

Until recently, to compute wave fields in inhomogeneous anisotropic media by the ray method it was necessary to specify a special isotropic layer, in which the source generating the considered waves was situated. Although the first theoretical steps were made a decade ago (see e.g., HANYGA, 1984), the first attempts to perform ray calculations of the wave fields or the radiation patterns generated by point sources in inhomogeneous anisotropic media were made only recently (BEN-MENAHEM *et al.*, 1991; GAJEWSKI, 1993). An important part of the ray formulae

[1] Geophysical Institute, Academy of Sciences of Czech Republic, Boční II, Praha 4, Czech Republic.
[2] PPPG, Universidade Federal da Bahia, Rua Caetano Moura 123, Federação, 40.210.350 Salvador, Brazil.

for the radiation of general types of point sources is the ray Green function. The ray Green function represents the leading term of the expansion of the exact Green function into the ray series. Formulae for the ray Green function for inhomogeneous anisotropic media were presented by several authors (see e.g., ČERVENÝ, 1990; BEN-MENAHEM *et al.*, 1991; KENDALL *et al.*, 1992). In the aforementioned papers, the authors concentrated on anisotropic media in which the slowness surfaces of all waves were convex. In these cases, the group velocity surfaces were smooth, single-valued surfaces.

In this article we extend the work of the previous authors to any type of anisotropy. Since we use the ray method, our results are, of course, invalid at caustic regions. In our formulae for the displacement vector of a single elementary wave due to various types of point sources, we separate the effects which are connected with a considered type of source from the effects connected with the geometrical spreading. We introduce the so-called directivity function, which is, in fact, the spreading-free amplitude at the source. It only depends on the type and orientation of the source and on the parameters of the medium exactly at the point source. The effects of the structure surrounding the source on the propagation of the generated waves are described by the so-called relative geometrical spreading (see e.g., ČERVENÝ, 1995), which is a reciprocal quantity. For evaluation of the relative geometrical spreading we use the dynamic ray tracing with specially chosen initial conditions, which removes artificial problems of indefinable ray amplitudes in certain directions. In this way, the radiation pattern defined as a modulus of the amplitude of the displacement vector of a generated elementary, harmonic wave can be expressed as an absolute value of the ratio of the directivity function and the relative geometrical spreading. With the geometrical spreading known, the above formulation allows us to calculate very effectively the wave fields for arbitrary point sources with arbitrary orientations. This formulation can be straightforwardly extended to the calculation of ray synthetic seismograms due to point sources in layered inhomogeneous isotropic and/or anisotropic media.

In the first part of the paper, we derive the formulae for the displacement vector resulting from a point source in an inhomogeneous anisotropic medium. Certain specific problems related to this part are explained in the Appendices. In the second part, we present numerical examples, which show the effects of anisotropy on the directivity function, the geometrical spreading and the radiation pattern. Examples presented in this article are selected from an extensive numerical study performed by TELES (1995). In a simple numerical experiment simulating a VSP measurement, we demonstrate the effects of anisotropy on the ray synthetic seismograms generated by point sources located in homogeneous isotropic and anisotropic media.

Vector and component notations are used alternatively throughout the paper. In the case of component notation, Einstein summation convention is used. The following notation for partial derivatives with respect to spatial coordinates is used: $u_{i,jk} = \partial^2 u_i / \partial x_j \partial x_k$.

2. Basic Formulae

Radiation from point sources is described by the well-known formulae resulting from the representation theorems (see e.g., AKI and RICHARDS, 1980). In the frequency domain, for the point force sources, we have

$$u_i(x_m, \omega) = G_{in}(x_m, x_{om}, \omega) f_n(x_{om}, \omega) \tag{1a}$$

and for the moment point sources, we have

$$u_i(x_m, \omega) = G_{in,l}(x_m, x_{om}, \omega) M_{nl}(x_{om}, \omega). \tag{1b}$$

Here, $u_i(x_m, \omega)$ denotes the displacement vector at the point x_m. Symbols f_n and M_{nl} denote a point force and a point moment tensor, respectively. Function $G_{in}(x_m, x_{om}, \omega)$ is the time-harmonic elastodynamic Green function. It represents the i-th component of the displacement vector recorded at the point x_m due to the unit point force situated at the point x_{om} and oriented along the n-th Cartesian coordinate axis. The force radiates a harmonic wave with frequency ω. The Green function is the solution of the inhomogeneous elastodynamic equation

$$(c_{ijkl} G_{kn,l})_{,j} + \rho \omega^2 G_{in} = -\delta_{in} \delta(x_m - x_{om}). \tag{2}$$

Here $c_{ijkl} = c_{ijkl}(x_m)$ is the tensor of elastic parameters, $\rho = \rho(x_m)$ is the density, δ_{in} denotes the Kronecker symbol and δ the Dirac delta function. From equations (1), we can discern that for the calculation of radiation from point sources we must know the Green function. We shall seek the solution of the elastodynamic equation (2) for inhomogeneous media using the ray method. We shall call the zero-order ray approximation of the Green function the *ray Green function* and denote it $G^R_{in}(x_m, x_{om}, \omega)$.

2.1. Ray Green Function

In the ray method a solution of the elastodynamic equation is sought in the form of a superposition of contributions of individual elementary waves. In this way, the ray Green function can be expressed as a superposition of elementary ray Green functions (see e.g., ČERVENÝ *et al.*, 1987). In the following we concentrate on one of the elementary ray Green functions and for simplicity we also call it the ray Green function.

In the ray method the solution of the inhomogeneous elastodynamic equation (2) is determined by solving the corresponding homogeneous elastodynamic equation, which must satisfy the initial conditions corresponding to the considered source. The zero-order ray approximation of the solution of the homogeneous elastodynamic equation along a selected ray can be written in the following form (see e.g., ČERVENÝ *et al.*, 1977):

$$u_i(x_m, \omega) = A(x_m) g_i(x_m) \exp[-i\omega(t - \tau(x_m))]. \tag{3}$$

In (3), $A(x_m)$ is the scalar ray amplitude and $g_i(x_m)$ is the unit polarization vector of the considered wave. Function $\tau(x_m)$ is the phase function or eikonal. The scalar amplitude is given by the formula

$$A(x_m) = A(x_{om})\left[\frac{\rho(x_{om})c(x_{om})\Omega_M(x_{om})}{\rho(x_m)c(x_m)\Omega_M(x_m)}\right]^{1/2}. \tag{4}$$

Symbol c in (4) denotes the phase velocity. Quantity Ω_M is related to the relative geometrical spreading $|\Omega_M|$ obtained from the dynamic ray tracing with especially chosen initial conditions (A.5), see Appendix A.

Equation (4) expresses the preservation of the quantity

$$A(x_m)[\rho(x_m)c(x_m)\Omega_M(x_m)]^{1/2}$$

along the selected ray. Equation (4) can be used for the continuation of the ray wave field from the point x_{om} to the point x_m along the selected ray. It cannot be used, however, in the above form, for the calculation of the wave field from a point source since as we approach the point source, the quantity $\Omega_M(x_m)$ goes to zero and the scalar amplitude $A(x_m)$ goes to infinity with the same speed (BLEISTEIN, 1984). Since for nonzero $\Omega_M(x_m)$ the amplitude $A(x_m)$ along the ray must be finite and ρ and c are also finite, it is obvious that the quantity

$$A(x_m)\Omega_M^{1/2}(x_m)$$

must be finite everywhere including the limiting case: the source. Therefore, we introduce a quantity $D(x_{om}, \gamma_1, \gamma_2)$ such that

$$D(x_{om}, \gamma_1, \gamma_2) = \lim_{x_m \to x_{om}} A(x_m)\Omega_M^{1/2}(x_m),$$

where the limit is performed along the ray specified by the ray parameters γ_1, γ_2. We call the quantity $D(x_{om}, \gamma_1, \gamma_2)$ the *directivity function*. We can see that we can understand $D(x_{om}, \gamma_1, \gamma_2)$ as the spreading-free amplitude at the source. If the directivity function is constant, we speak of *uniform* radiation, i.e., the radiation is the same to all directions. Here we are interested in the ray Green function. Therefore, we look for the directivity of the single force, which is not uniform.

Let us consider a unit force oriented along, say, the x_3 axis. It has the direction and size of the unit base vector $\vec{i}_3$ of the Cartesian coordinate system, i.e., $f_i = \delta_{i3}$. Let us further consider the polarization vector $g_i(x_{om})$ of the studied wave at the source. The contribution of the single force to the direction specified by $g_i(x_{om})$ is proportional to the projection of the polarization vector to the force $\vec{f}$, $\vec{g}(x_{om})\vec{f} = g_3(x_{om})$. The directivity function of the vertical unit single force can thus be written

$$D(x_{om}, \gamma_1, \gamma_2) = Cg_3(x_{om}), \tag{5}$$

where C is an unknown factor of proportionality. The formal relation for the

component $G_{i3}^R(x_m, x_{om}, \omega)$ of the ray Green function can be thus written as

$$G_{i3}^R = C\left[\frac{\rho(x_{om})c(x_{om})}{\rho(x_m)c(x_m)\Omega_M(x_m)}\right]^{1/2} g_3(x_{om})g_i(x_m)\exp[-i\omega(t-\tau(x_m))]. \tag{6}$$

It remains to determine the factor of proportionality C in eq. (6). It can be determined by matching eq. (6) with the G_{i3}^H component of the asymptotic Green function for a homogeneous anisotropic medium as the source is approached (BLEISTEIN, 1984; KENDALL *et al.*, 1992). For matching we can choose from a variety of formulae derived by various authors (see e.g., BUCHWALD, 1959; KOSEVICH and NATSIK, 1964; BURRIDGE, 1967; YEATTS, 1984; ČERVENÝ, 1995). In our notation, such a formula reads

$$G_{i3}^H = \frac{g_i g_3\, e^{-i\omega(t-r/v)}}{4\pi\rho v K^{1/2} r} = \frac{g_i g_3\, e^{i(\pi/2)k_S}\, e^{-i\omega(t-r/v)}}{4\pi\rho v |K|^{1/2} r}. \tag{7}$$

Here r is the distance between the source and an observer, v denotes the group velocity. The symbol K denotes the Gaussian curvature of the slowness surface in the direction specified by the slowness vector of the considered wave. It can be expressed as a product of the principal curvatures k_1 and k_2. We call the quantity k_S in (7) the *index of the source*. The index of the source can attain the values 0, 1 and 2 in the following situations:

$$\begin{aligned} &k_S = 0 \quad \text{if} \quad k_1 < 0, \quad k_2 < 0, \\ &k_S = 1 \quad \text{if} \quad k_1 < 0, \quad k_2 > 0 \quad \text{or} \quad k_1 > 0, \quad k_2 < 0, \\ &k_S = 2 \quad \text{if} \quad k_1 > 0, \quad k_2 > 0. \end{aligned} \tag{8}$$

We can see that $k_S = 0$ if the slowness surface at the source is convex for a given direction of the slowness vector (this is always the case in isotropic media where the slowness surface is a sphere), $k_S = 1$ if the slowness surface is saddle-shaped and $k_S = 2$ if it is concave. If one or both principal curvatures are zero, formula (7) becomes singular (corresponding points on the slowness surface are called parabolic points) and eq. (7) cannot be used without a modification.

Let us specify the above formula (6) for the component G_{i3}^R of the ray Green function for a homogeneous medium. We obtain

$$G_{i3}^R = \frac{C g_i g_3\, e^{-i\omega(t-r/v)}}{\Omega_M^{1/2}}.$$

If we insert formula (B.2) derived in Appendix B,

$$\Omega_M = (v/c)^2 K r^2,$$

into the above formula, G_{i3}^R can be rewritten as

$$G_{i3}^R = \frac{C c g_i g_3\, e^{-i\omega(t-r/v)}}{v K^{1/2} r}. \tag{9}$$

A comparison of eq. (9) with (7) yields

$$C = \frac{1}{4\pi\rho c}.$$

The formula for the directivity function of the G_{i3}^R component of the ray Green function corresponding to any of the three waves, which can propagate in anisotropic media, can be thus written as

$$D(x_{om}, \gamma_1, \gamma_2) = \frac{g_3(x_{om})}{4\pi\rho(x_{om})c(x_{om})}. \tag{10}$$

We can repeat the above procedure for the remaining components of the ray Green function, G_{i1}^R and G_{i2}^R. Since the factor of proportionality C is the same for any component, we can write the final formula for the time-harmonic ray Green function as follows

$$G_{in}^R = \frac{g_i(x_m)g_n(x_{om})\, e^{-i(\pi/2)k(x_{om}, x_m)}\, e^{i(\pi/2)k_S}\, e^{-i\omega(t-r/v)}}{4\pi[\rho(x_{om})\rho(x_m)c(x_{om})c(x_m)|\Omega_M(x_m)|]^{1/2}}. \tag{11}$$

Here k_S is the above introduced index of the source and $k = k(x_{om}, x_m)$ is the *index of ray trajectory*, which equals the number of first-order caustics encountered by the considered wave moving from the source to the point x_m. Note that the index of the source causes a shift with a sign opposite that of the index of ray trajectory.

The formula (11) is applicable to arbitrary inhomogeneous anisotropic media, regardless if the slowness surface is convex or concave for a given direction. In the directions corresponding to the transition from a convex to a concave part of the slowness surface, the geometrical spreading (and the Gaussian curvature of the slowness surface as well) become zero and the formula (11) does not work. As in the case of any other singularity of the ray method, the region of inapplicability of (11) is frequency dependent. Let us note that similar formulae for anisotropic media with convex slowness surfaces have been found by ČERVENÝ (1990), BEN-MENAHEM *et al.* (1991) and KENDALL *et al.* (1992).

2.2. Radiation from Point Sources

Let us return to formulae (1) and let us transform them into the time domain. Using eq. (11), we get

$$u_i(x_m, t) = g_i(x_m)\left[\frac{\rho(x_{om})c(x_{om})}{\rho(x_m)c(x_m)}\right]^{1/2} \frac{Df^{(A)}(t-\tau(x_m))}{|\Omega_M(x_m)|^{1/2}} \exp\left[i\frac{\pi}{2}k_s - i\frac{\pi}{2}k(x_{om}, x_m)\right]. \tag{12}$$

The real part of the above formula represents an elementary ray seismogram

generated by a point source. Symbol $f^{(A)}$ denotes an analytic signal which has the form

$$f^{(A)}(\theta) = F(\theta)$$

for the force source and

$$f^{(A)}(\theta) = F'(\theta)$$

for the moment tensor source. The prime denotes the derivative with respect to the argument. In both cases the function $F(\theta)$ is a high-frequency analytic signal corresponding to the source-time function. Quantity $D = D(x_{om}, \gamma_1, \gamma_2)$ in eq. (12) is the directivity function of the corresponding source. In the case of the force source it has the form

$$D(x_{om}, \gamma_1, \gamma_2) = \frac{g_n(x_{om}) f_n}{4\pi\rho(x_{om})c(x_{om})} \tag{13a}$$

and in the case of the moment tensor source it has the form

$$D(x_{om}, \gamma_1, \gamma_2) = \frac{g_n(x_{om}) M_{nl} p_l(x_{om})}{4\pi\rho(x_{om})c(x_{om})}. \tag{13b}$$

Here again, f_n is the force and M_{nl} is the moment tensor. Symbol $p_l(x_{om})$ denotes the slowness vector at the source. We note that the directivity function for the moment tensor source can also be used for the explosive source if the moment tensor is specified as $M_{nl} = M_o \delta_{nl}$, where M_o is a constant factor. For dislocation sources M_{nl} must be specified as

$$M_{nl} = [u_i] n_j c_{ijnl},$$

(see AKI and RICHARDS, 1980; TSVANKIN and CHESNOKOV, 1990b). Here $[u_i]$ is the dislocation (the displacement discontinuity) across the fault specified by the normal n_i. We note that in general anisotropic media the structure of the moment tensor can be more complicated than in isotropic media (see e.g., KAWASAKI and TANIMOTO, 1981).

The generalization of eq. (12) for layered media is straightforward (see e.g., ČERVENÝ *et al.*, 1977; ČERVENÝ, 1995).

In the following we present results of the numerical study of effects of anisotropy on the directivity function, the geometrical spreading and the radiation pattern. The radiation pattern $P(x_{om}, \gamma_1, \gamma_2)$ of the source at x_{om} is defined as

$$P(x_{om}, \gamma_1, \gamma_2) = (AA^*)^{1/2},$$

where A is the scalar ray amplitude and the asterisk denotes complex conjugacy. The ray amplitude A is specified on a unit sphere with its center at the source. The

radiation pattern is thus calculated from the formula

$$P(x_{om}, \gamma_1, \gamma_2) = \left| \frac{D(x_{om}, \gamma_1, \gamma_2)}{\Omega_M(x_m)^{1/2}} \right|. \tag{14}$$

We can see that the radiation pattern of the source is affected by two factors: the directivity of the source and the geometrical spreading. As we shall see, the geometrical spreading can have quite a strong angular dependence even in homogeneous anisotropic media. In homogeneous isotropic media the geometrical spreading does not depend on the direction and thus the directivity function and the radiation pattern differ only by a multiplicative factor.

3. Numerical Examples

We consider a general Cartesian coordinate system with the axes x and y positioned in the horizontal plane and the z axis vertical with its positive part pointing down. In the following examples the directivity function is displayed in [m^3/s], the modified spreading in [10^{12} m^4/s^2] and the radiation pattern in [10^{-6} m]. The strength of the considered explosive sources is always 10^6 N m, of the force sources 10^6 N. For estimation of the effects of anisotropy we also study the radiation from point sources situated in an equivalent isotropic medium. The velocities in the equivalent isotropic medium are found by averaging corresponding maximum and minimum phase velocities.

3.1. Orthorhombic Model

In this section we study the effects of the orthorhombic olivine on the directivity function, the geometrical spreading and the radiation pattern. The model, originally proposed by KUMAZAWA and ANDERSON (1969), was used to calculate the radiation pattern by, for example, TSVANKIN and CHESNOKOV (1990a,b), BEN-MENAHEM *et al.* (1991) and GAJEWSKI (1993). The model is homogeneous and it is described by the following matrix of density normalized elastic parameters

$$\begin{pmatrix} 98.18 & 17.88 & 23.94 & 0.00 & 0.00 & 0.00 \\ & 60.00 & 23.64 & 0.00 & 0.00 & 0.00 \\ & & 75.46 & 0.00 & 0.00 & 0.00 \\ & & & 20.21 & 0.00 & 0.00 \\ & & & & 24.55 & 0.00 \\ & & & & & 24.03 \end{pmatrix},$$

specified in 10^6 (m/s)^2 and by the density of 3300 kg/m^3. The degree of anisotropy of qP waves is about 22%, and the degree of anisotropy of both qS waves is about

19%. The axes of symmetry of the model coincide with axes of the general Cartesian coordinate system. The P- and S-wave velocities of the equivalent isotropic medium are 8.8 and 5.0 km/s respectively.

Figure 1 shows the sections of the slowness surfaces (on the LHS) and the group velocity surfaces (on the RHS) corresponding to the above matrix of elastic parameters with the xy (the upper line), xz (the middle line) and yz (the bottom line) planes. It follows from eq. (B.2) that the geometrical spreading in a homogeneous model is proportional to the curvature of the slowness surface at the source. Keeping this relation in mind when inspecting the left column of Figure 1, we can roughly identify the directions in which the curvature is zero and thus the ray amplitude tends to infinity. Similarly, we can roughly identify the directions of large curvature and thus of small ray amplitudes. These rough estimates are confirmed in Figure 2 which shows the relative geometrical spreading $|\Omega_M|$ measured on a unit sphere around the source. The sections exhibit rays shot with equally spaced initial angles of the slowness vector. The length of the rays indicates the corresponding value of spreading. The spreading is greater (and the ray amplitudes are smaller) in the directions in which the density of rays is smaller and *vice versa*. Figure 2 illustrates that the relative geometrical spreading of the qP wave exceeds that of the qS waves. This occurs because in the formula for the relative geometrical spreading, the distance r is scaled by a factor proportional to the group velocity v, see eq. (B.2). We can also see that for all the studied waves and most considered directions, the sections of the spreading deviate from circles which would be observed in isotropic media.

The slowness of the qP wave displays smooth variations, therefore, the geometrical spreading also varies smoothly. The situation with the $qS1$ wave is different. The form of the slowness surface in the sections xy and xz is rather complicated and this is reflected in the complex form of the geometrical spreading. For some directions the spreading drops to zero (due to the finite step in the initial angles of the slowness vectors the zeros are not clearly seen in Figure 2), in other directions it reaches extraordinarily large values. In the yz section, however, the spreading of the $qS1$ wave has a form close to the form in isotropic media. With the exception of the xy section, the geometrical spreading of the $qS2$ wave is finite and nonzero.

The geometrical spreading discussed above is the same for any type of the source. We now study the directivity function, see eq. (13). Its form generally depends on the type and orientation of the source.

Figure 3 exhibits a 3-D display of the directivity functions resulting from an explosive point source situated in the above specified orthorhombic olivine. Directivity functions of the qP, $qS1$ and $qS2$ waves are shown from top to bottom. We can see that the explosive source generates not only the qP wave as in an isotropic medium but also relatively strong qS waves. The directivity function of the qP wave deviates only slightly from a sphere, which would be generated in an isotropic

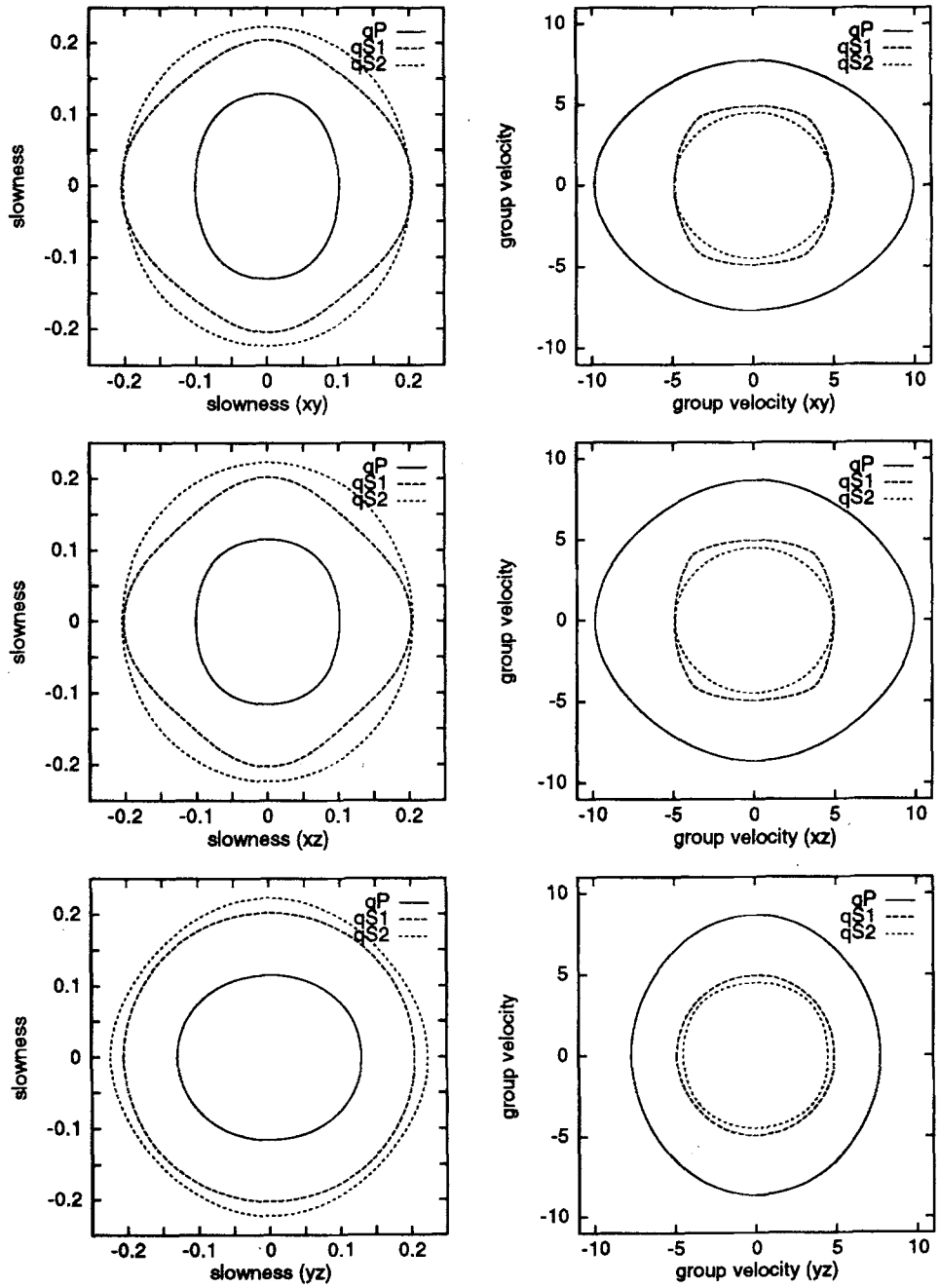

Figure 1
Sections of the slowness surfaces (left) and of the group velocity surfaces (right) of the orthorhombic olivine with *xy* (top), *xz* (middle) and *yz* (bottom) planes.

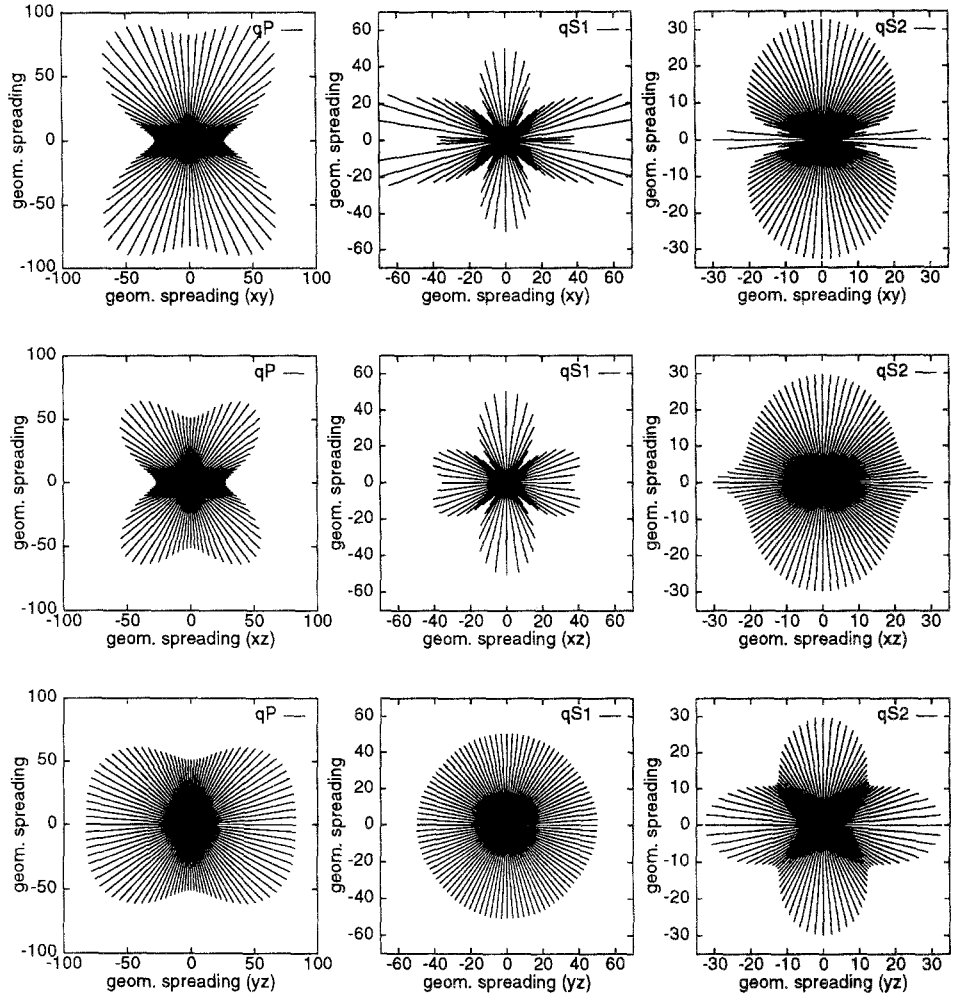

Figure 2
Sections of the geometrical spreading measured at a unit distance from the source situated in the orthorhombic olivine model for qP (left), $qS1$ (middle) and $qS2$ (right) waves. Sections with xy (top), xz (middle) and yz (bottom) planes are shown.

medium. The forms of the directivity functions of the $qS1$ and $qS2$ waves are, however, more complicated. We can see that the directivity function of the slower of the generated qS waves is weaker than the faster one. We take note that the directivity function of the $qS1$ wave is zero in the yz section while the directivity of the $qS2$ wave is zero in the xy and xz sections. In the remaining principal sections the directivity functions have a four-lobed form.

Figure 4 shows the xz section of the directivity function, of the geometrical spreading and of the radiation pattern of the qP and $qS1$ wave due to an explosive

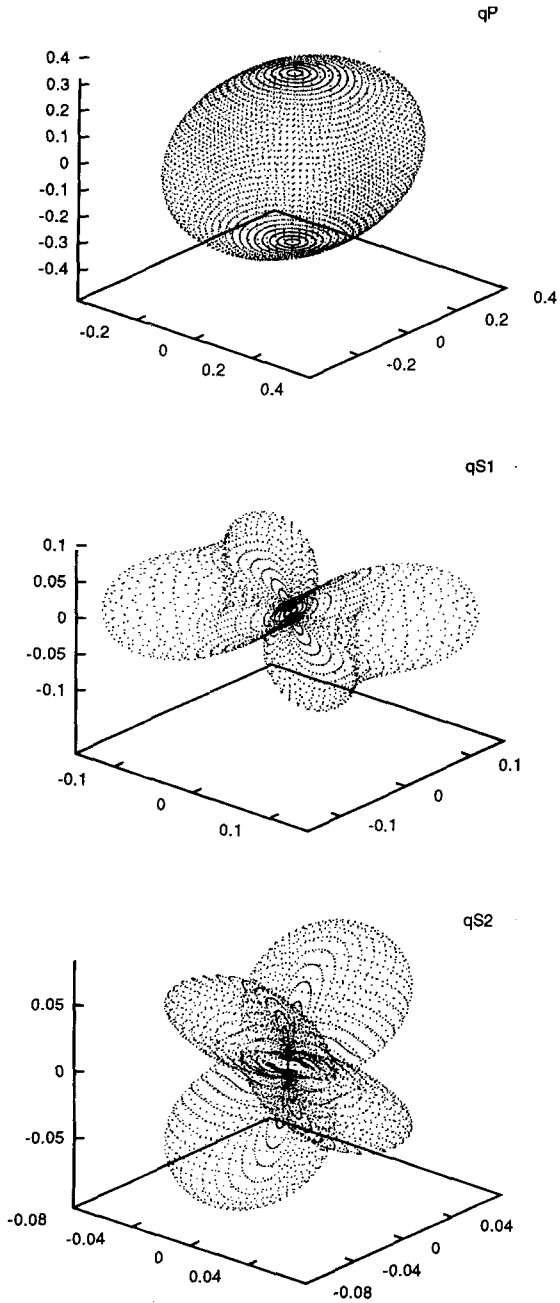

Figure 3
Directivity functions of qP (top), $qS1$ (middle) and $qS2$ (bottom) waves generated by an explosive source situated in the orthorhombic olivine model.

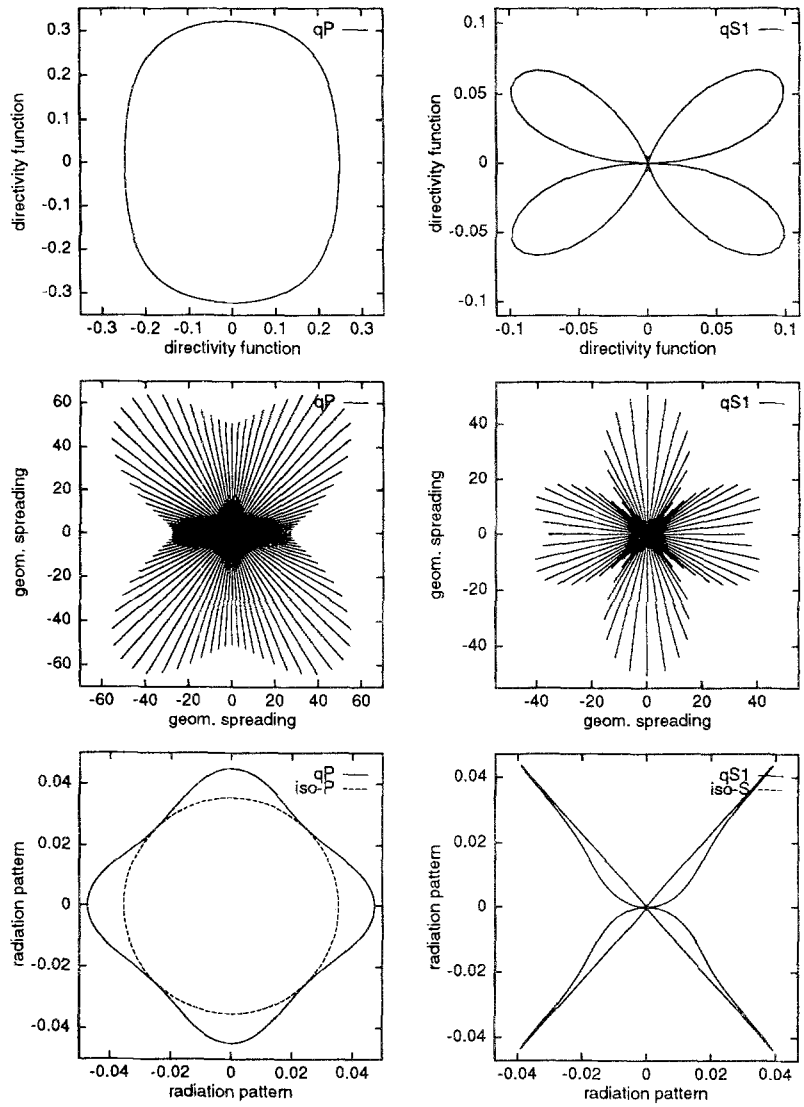

Figure 4

The xz sections of the directivity function (top), of the geometrical spreading (middle) and of the radiation pattern (bottom) of the qP (left) and $qS1$ (right) waves generated by an explosive source situated in the orthorhombic olivine model. The directivity function and the radiation pattern of the $qS2$ wave in the xz section are zero.

point source situated in the orthorhombic model. The radiation pattern is defined by eq. (14). The pictures related to the $qS2$ wave are not shown because, as stated above, the directivity function and thus also the radiation pattern, are zero in the xz section. The radiation pattern corresponding to the equivalent isotropic medium is shown by a dashed line. While in the case of the qP wave the radiation pattern

is mostly affected by the geometrical spreading, in the case of the $qS1$ wave the effects of the directivity function and of the geometrical spreading combine. Although the bottom frame of Figure 4 displays seemingly finite pattern of the $qS1$ wave, the lobes, in fact, reach infinity (their finite extent is caused by the evaluation of the radiation pattern at a discrete set of radiation angles). The infinite value of the radiation pattern is caused by the zero value of the geometrical spreading (zero value of the Gaussian curvature of the slowness surface) and represents a typical singularity of the ray method. It could be removed if a generalization of the ray method such as the method of summation of Gaussian beams is used. See also a discussion of this problem in BEN-MENAHEM *et al.* (1991) and GAJEWSKI (1993).

Figure 5 shows the same as Figure 4 but for the section xy. In this section the geometrical spreading is always nonzero and, therefore, the radiation pattern is finite. Note that this time only the pictures of the $qS2$ wave are shown. The directivity function of the $qS1$ wave in the section xy is zero and thus the radiation pattern is also zero.

Figures 6 and 7 display the xz and yz sections of the directivity function, of the geometrical spreading and of the radiation pattern deriving from a vertical force source set in the orthorhombic model. Similarly as in Figures 4 and 5, the radiation patterns of the $qS2$ wave in the xz section and of the $qS1$ wave in the yz section are zero. The effect of anisotropy on the directivity function is relatively weak. The anisotropy affects more significantly the geometrical spreading. In the xz section the geometrical spreading of the $qS1$ wave is zero in 4 directions, which again leads to the singular behavior of the radiation pattern. In the vicinity of these directions the ray results must be considered with care (see GAJEWSKI, 1993).

3.2. Hexagonally Symmetric Model

In this section we study the effects of a homogeneous anisotropic model with hexagonal symmetry on the radiation of point sources. As a model we consider one of the models derived by SHEARER and CHAPMAN (1989) for effectively anisotropic media using HUDSON's (1981) theory. The matrix of density normalized elastic parameters with the axis of symmetry oriented along the x axis of the general Cartesian coordinate system has the form:

$$\begin{bmatrix} 11.91 & 4.40 & 4.40 & 0.00 & 0.00 & 0.00 \\ & 19.11 & 6.35 & 0.00 & 0.00 & 0.00 \\ & & 19.11 & 0.00 & 0.00 & 0.00 \\ & & & 6.38 & 0.00 & 0.00 \\ & & & & 5.10 & 0.00 \\ & & & & & 5.10 \end{bmatrix}.$$

The density is 1000 kg/m^3. The model displays a strong qP wave anisotropy of

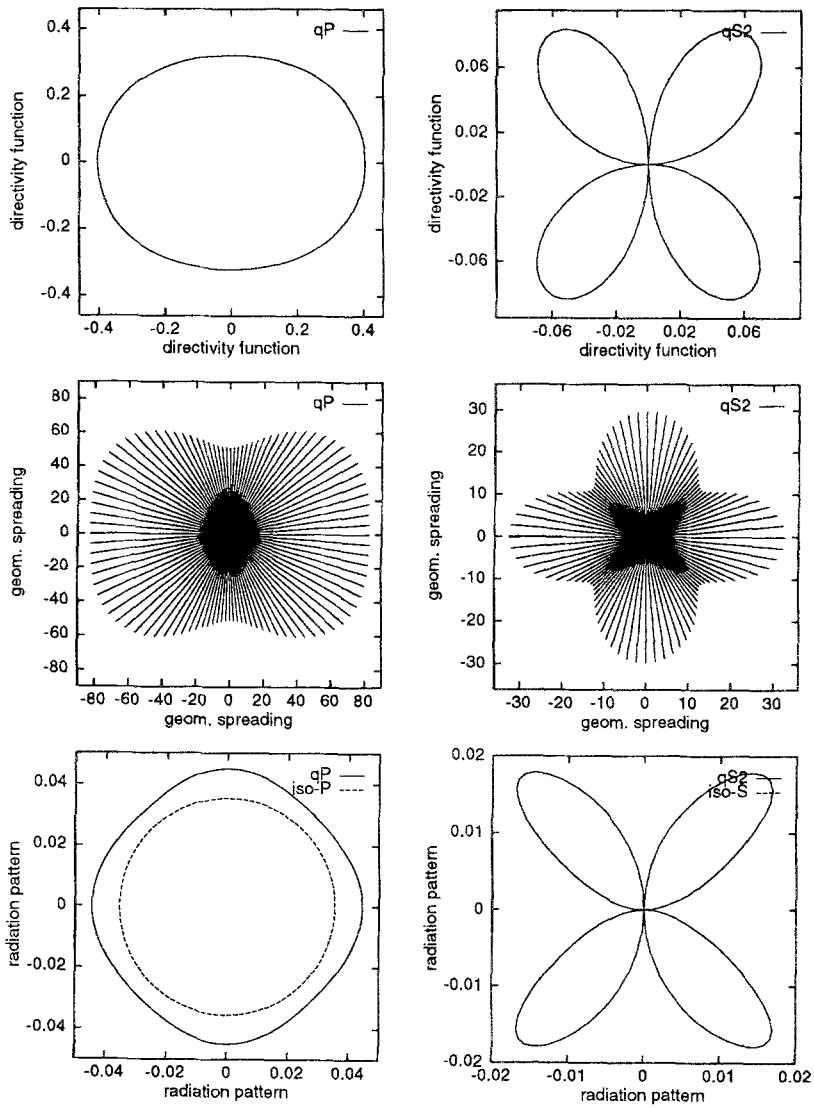

Figure 5
The same as in Figure 4 but for the xy section.

about 20%, the anisotropy of the qS waves being approximately 11%. The P- and S-wave velocities of the equivalent isotropic medium are 3.9 and 2.4 km/s, respectively.

In Section 3.1 we considered a model in which the axis of crystal symmetry coincided with the axes of the general Cartesian coordinate system. In this section, in addition to the effects of angular dependence of the properties of the medium, we also consider the effects of the general orientation of the axis of symmetry. In the

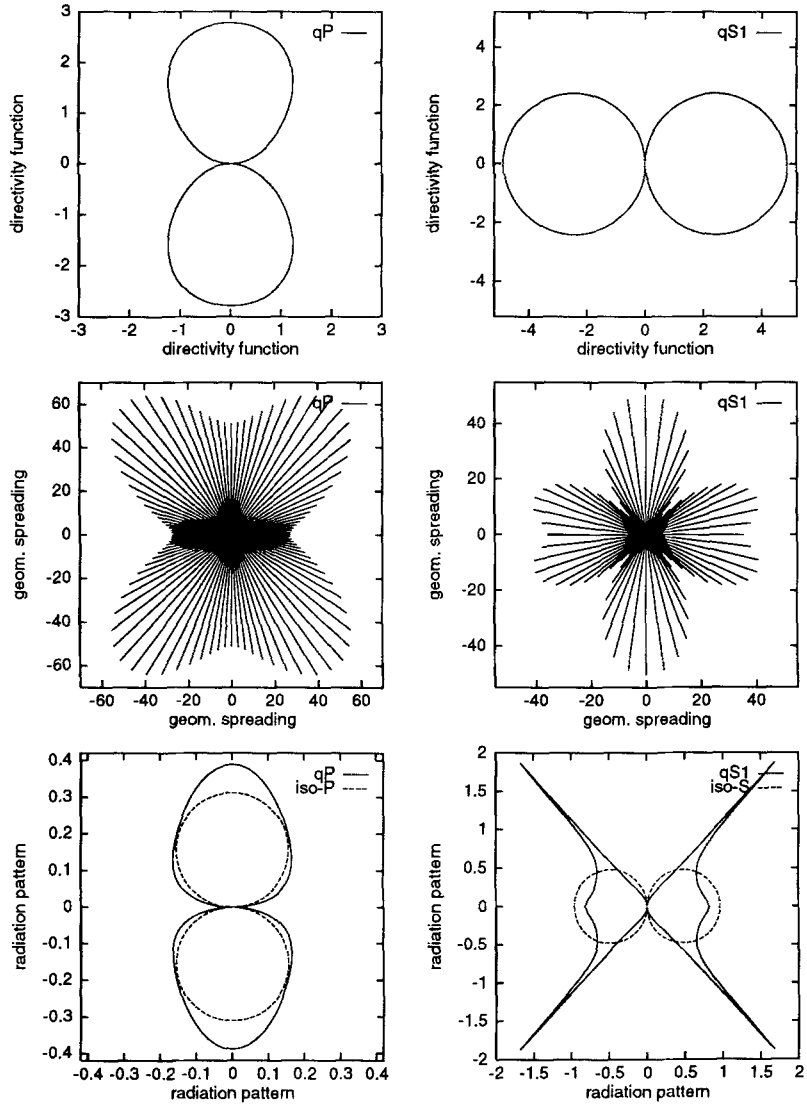

Figure 6
The same as in Figure 4 but for the vertical force source.

following considerations the axis of symmetry is tilted 30° from the horizontal plane and is located in the vertical plane which makes an angle of 30° with the xz plane.

Figure 8 shows sections of the slowness surface and the group velocity surface of all three waves with the xy and xz planes and with the plane of symmetry. We can see that in this case, the slowness surfaces of all three waves are very regular, therefore, we can expect a standard behavior of the quantities we study. The $qS2$ wave is the slowest wave in all directions.

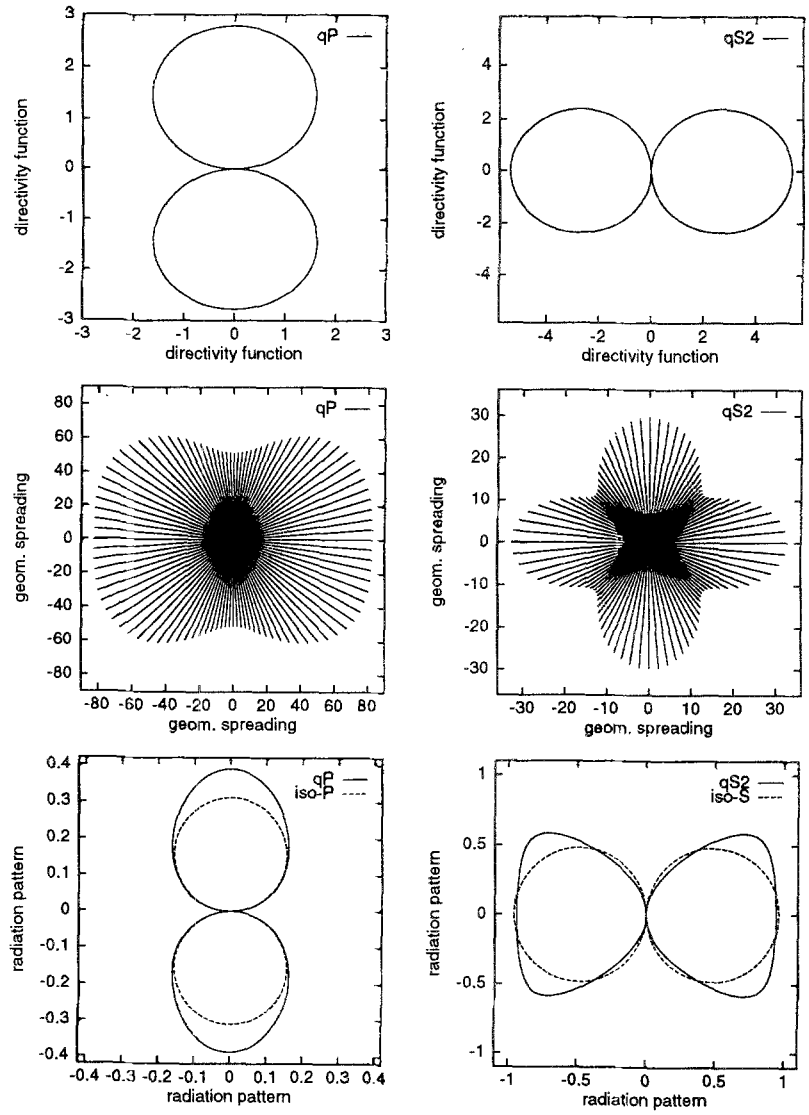

Figure 7
The same as in Figure 4 but for the xy section and the vertical force source.

Figure 9 displays the xz sections of the directivity function, of the geometrical spreading and of the radiation pattern of the qP and $qS2$ wave due to an explosive source. The directivity function and the radiation pattern of the $qS1$ wave are zero. Notably it is always the case in hexagonally symmetric media that only one qS wave is generated by an explosive source. Polarization vector of one of the qS waves is always perpendicular to the plane containing the axis of symmetry and the corresponding slowness vector. If the axis of symmetry were vertical, such a qS

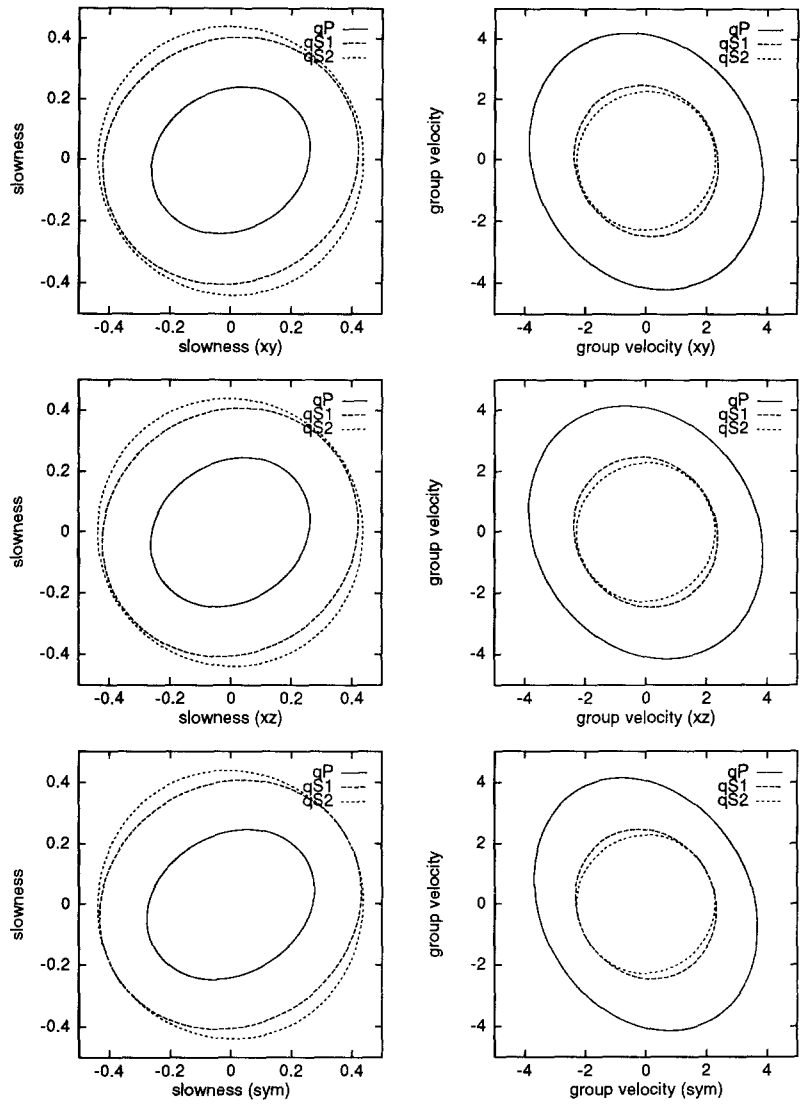

Figure 8
Sections of the slowness surfaces (left) and of the group velocity surfaces (right) of the hexagonally symmetric model with xy (top), xz (middle) and symmetry (bottom) planes.

wave could be referred to as an SH wave. Since the directivity function of the explosive source is proportional to the scalar product of the polarization vector and the corresponding slowness vector, the directivity function of the discussed qS wave is zero.

Another phenomenon of interest is the qP wave radiation. We can see that both the directivity function and the geometrical spreading exhibit relatively strong

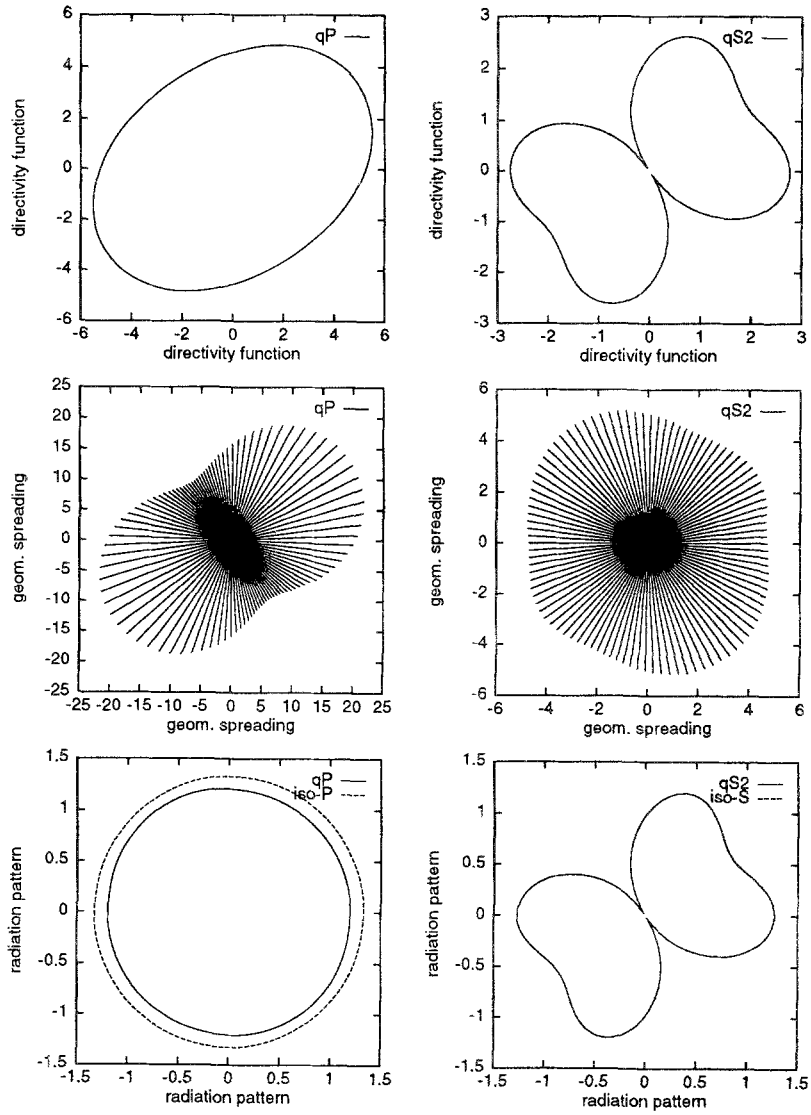

Figure 9

The xz sections of the directivity function (top), of the geometrical spreading (middle) and of the radiation pattern (bottom) of the qP (left) and $qS2$ (right) waves generated by an explosive source situated in the hexagonally symmetric model. The directivity function and the radiation pattern of the $qS1$ wave are zero.

angular dependence. Their combined effects, however, cancel each other and the resulting radiation pattern is practically uniform (dashed line again shows the radiation pattern of the source situated in the equivalent isotropic medium). The $qS2$ wave radiation is mostly influenced by the directivity function. We note that in contrast to the orthorhombic model, the radiation pattern of the $qS2$ wave is not

only limited to narrow bands of radiation angles and that it is nearly as strong as that of the qP wave. The fact that the radiation from the explosive source in the hexagonally symmetric medium is about 10 times stronger than in the orthorhombic medium, is caused by the used values of elastic parameters; compare the stiffness matrices for both cases.

Figure 10 again exhibits the xz sections of the directivity function, of the geometrical spreading and of the radiation pattern in the hexagonally symmetric medium, this time for the vertical force source. Notice that now all three waves are generated. We can see obvious distortions of the displayed patterns due to the

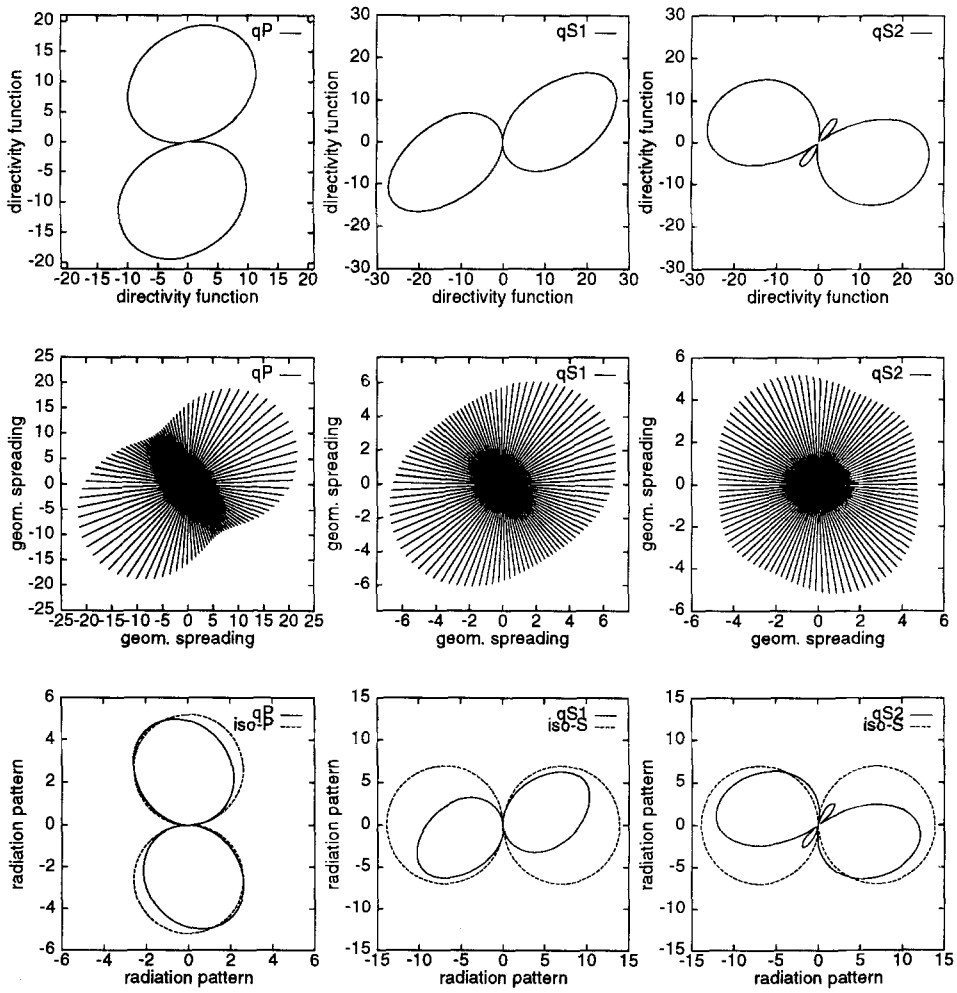

Figure 10
The xz sections of the directivity function (top), of the geometrical spreading (middle) and of the radiation pattern (bottom) of the qP (left), $qS1$ (middle) and $qS2$ (right) waves generated by the vertical force source situated in the hexagonally symmetric model.

general orientation of the axis of symmetry in space. Generally, the qP wave is less affected while in the $qS2$ case we can even observe a new phenomena, two additional lobes. They are caused by the fact that the polarization vector of the generated wave may become perpendicular to the generating force (see eq. (13a)) more frequently than in an isotropic case. Also note that the nodal line directions are slightly shifted because of the general orientation of the axis of symmetry.

We now consider a model of a homogeneous hexagonally symmetric medium with parameters described above, in which the axis of symmetry is horizontal and rotated in a horizontal plane by 40° from the x axis towards the y axis. In the terminology used in the study of cracked media (HUDSON, 1981; SHEARER and CHAPMAN, 1989) this means that we consider a system of vertical parallel cracks. In this model we perform the VSP experiment shown schematically in Figure 11. The profile connecting the source (S) with the vertical borehole and the borehole itself are situated in the xz plane. There are 13 three-component receivers located in the borehole in the depth range of 0.1–0.7 km with a step of 0.05 km. The distance of the source from the borehole is 0.5 km. As the source-time function we use the Gabor signal (see e.g., ČERVENÝ *et al.*, 1977), with a prevailing frequency of 50 Hz and the parameter $\gamma = 4$. The effects of the free surface on the source are not considered. Apart from seismograms generated by a point source situated in the anisotropic medium, we also generate seismograms for an equivalent isotropic medium.

In Figure 12, we present seismograms generated by an explosive source in the effective isotropic medium (left column) and in the hexagonally symmetric medium

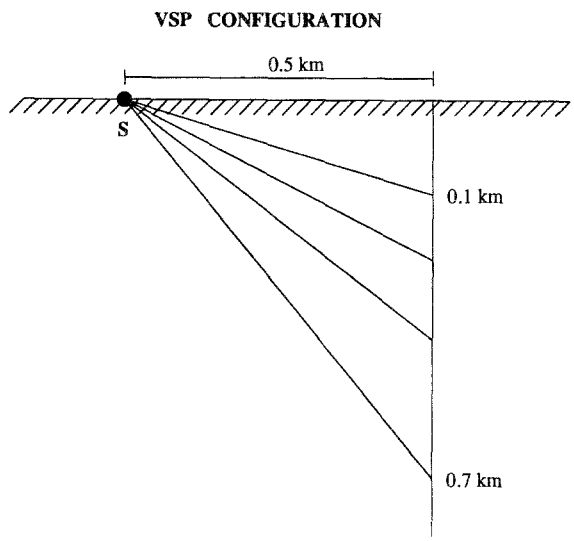

Figure 11
Schematic picture of the VSP experiment in the hexagonally symmetric model.

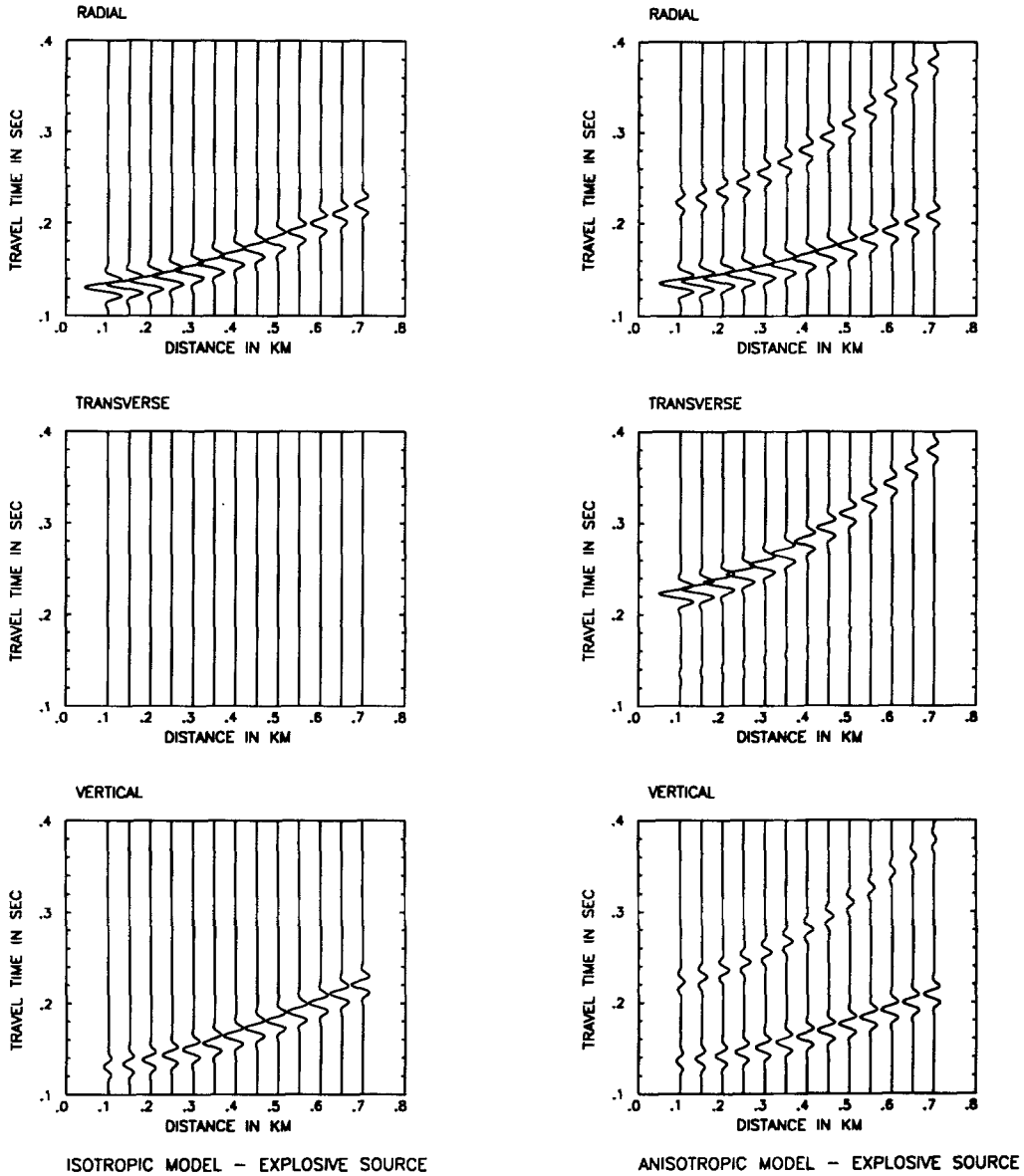

Figure 12
Ray synthetic seismograms for the VSP configuration shown in Figure 11. Left column: equivalent isotropic medium; right column: hexagonally symmetric medium. From top to bottom: radial, transverse and vertical components.

(right column). The first obvious difference between the two sets of seismograms, which are all scaled correspondingly, is missing energy on the transverse component of the isotropic model. Another difference is the missing second arrival in the isotropic model. The second arrival in the anisotropic model corresponds to the

$qS2$ wave, the slowest wave in the model. As mentioned above, the $qS1$ wave is not generated. We can see that, especially at shallow receivers, the $qS2$ wave can compete in strength with the qP wave. Another interesting phenomenon is weak qP wave arrival on the transverse component for shallow receivers.

The above-mentioned phenomena can be seen even better in Figure 13, which shows particle motion diagrams for selected receivers (0.1, 0.3, 0.55 and 0.7 km).

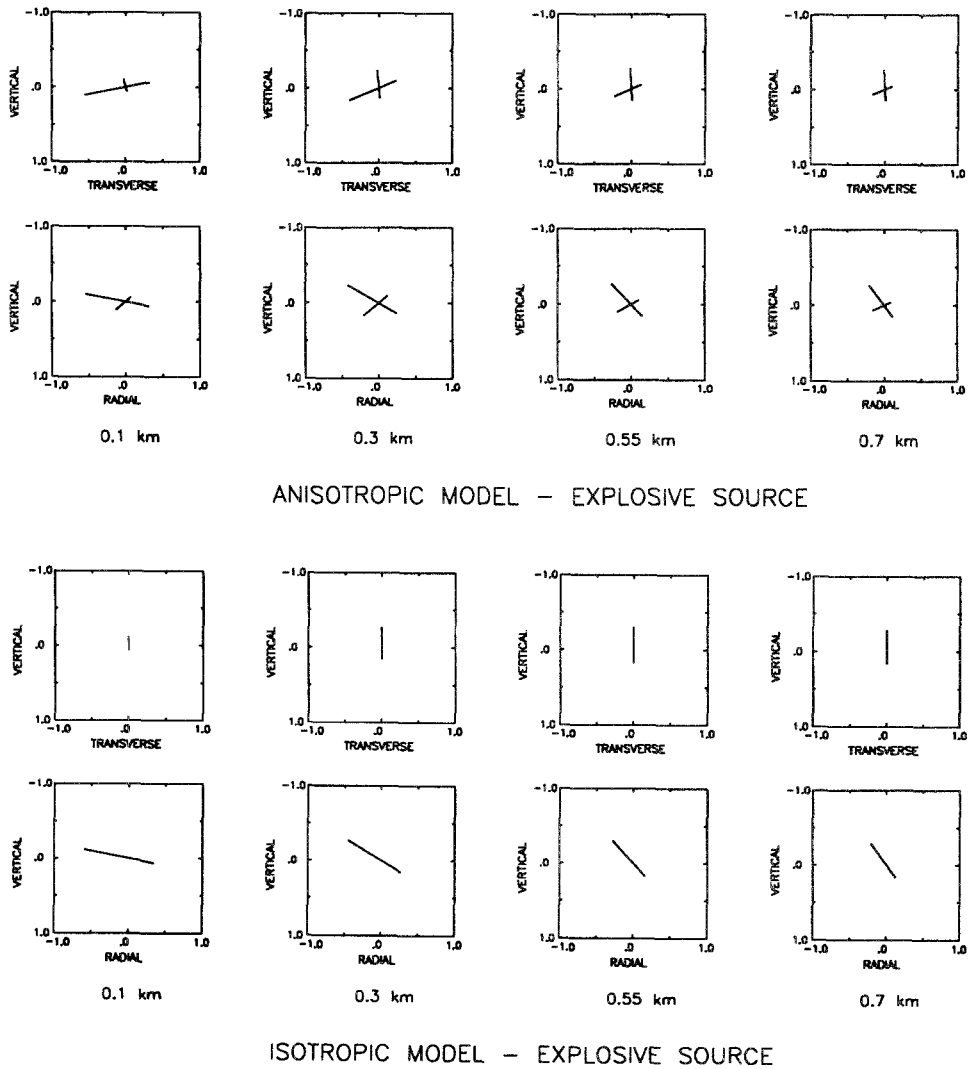

Figure 13
Ray particle motion diagrams for selected receivers, from left to right 0.1, 0.3, 0.55 and 0.7 km of depth in the VSP experiment shown in Figure 11. Upper 8 frames: hexagonally symmetric model; lower 8 frames: equivalent isotropic model.

The used time window corresponds to that used in seismograms presented in the preceding figure. The same amplification factor is applied in all figures. In the upper set, corresponding to the anisotropic model, we can see a strong $qS2$ wave at the first two receivers. Although the medium is anisotropic, the polarization of generated waves is strictly linear. This is a consequence of the above-mentioned fact that

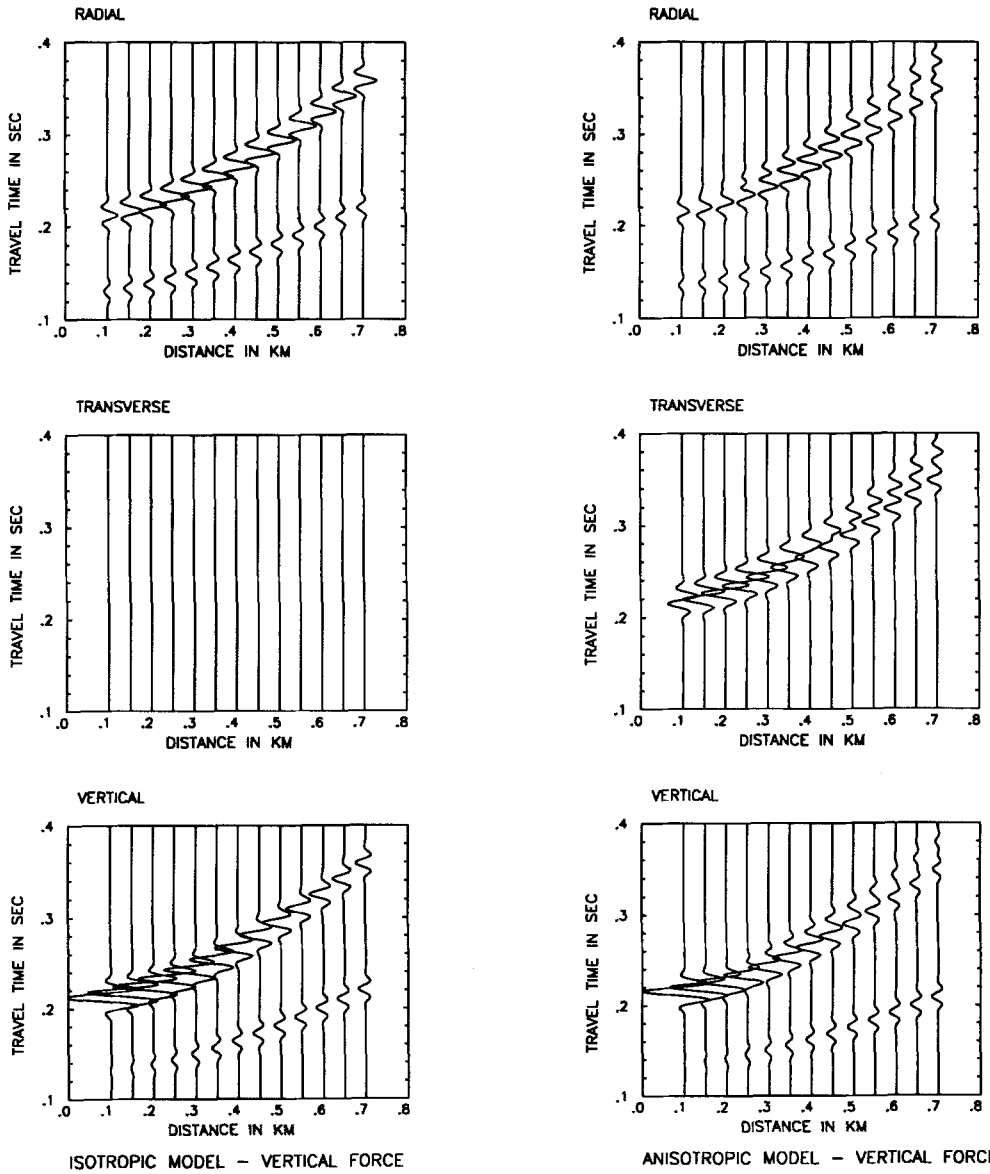

Figure 14
As in Figure 12 but for the vertical force source.

an explosive source in a hexagonally symmetric medium generates only a single qS wave.

Figure 14 shows ray synthetic seismograms for the same configuration as in Figure 12 but with the explosive source substituted by the vertical force source. Similar to Figure 12 there is no energy on the transverse component for the source situated in the equivalent isotropic medium, see the left column. In the right column, which shows seismograms for the source situated in the anisotropic medium, we can observe two rather strong qS waves while in the isotropic case a

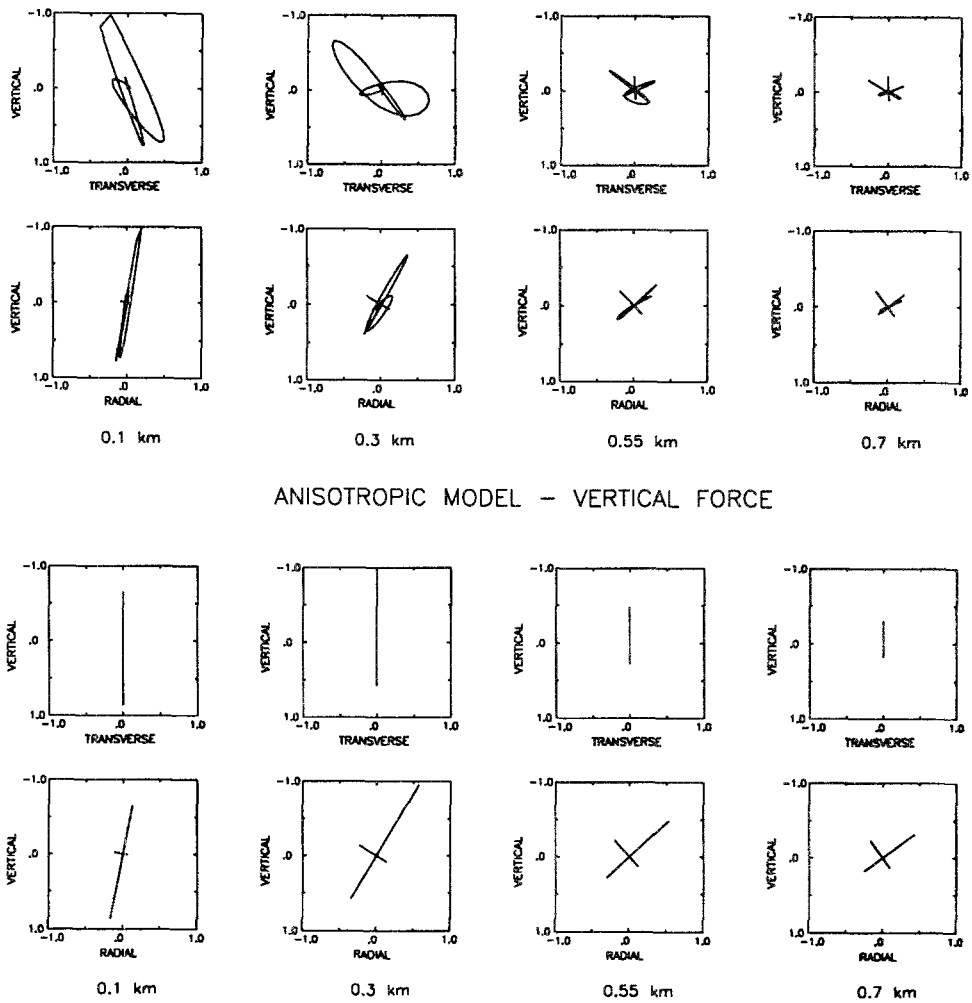

Figure 15
As in Figure 13 but for the vertical force source.

single S wave can be observed. We can see that both qS waves interfere at shallow receivers and separate continuously with the increasing depth of a receiver. The interference leads to quasi-elliptical polarization of qS waves, which can be clearly seen in the upper part of Figure 15. As in Figure 13, the upper part shows particle motion diagrams for the source situated the anisotropic medium while the bottom part displays the same for the source situated in the equivalent isotropic medium.

4. *Conclusions*

A general formula for calculating the zero-order ray amplitude displacement vector generated by an arbitrary type of an arbitrarily oriented point source in an arbitrary unbounded inhomogeneous anisotropic medium was presented. In the specified case, anisotropy affects the displacement through two factors: the directivity function and the geometrical spreading. The former depends fully on the properties of the source and on the properties of the medium at the point of the source. The latter depends only on the parameters of the medium surrounding the source and it is independent of the type and orientation of the considered source. The directivity function is always finite. It can be zero in certain directions which correspond to the nodal lines of the studied source. The geometrical spreading can also be zero in certain directions, different from those for the directivity function. The zero values of the geometrical spreading indicate the existence of caustics. In contrast to isotropic media, in which caustics appear only as a consequence of structural properties, in anisotropic media the caustics can also be produced by the source itself. This occurs if the slowness surface of a qS wave has a flat part, i.e., whenever the radius of the curvature of the slowness surface becomes zero. The flat part can exist between convex parts (as in the examples studied in this paper) or between convex and concave parts. The latter case leads to loops in the group velocity surface.

Although the formulae derived in the article are applicable to any kind of anisotropy including anisotropy in which the slowness surface of one of the qS waves has concave parts, here, for simplicity, only numerical examples related to homogeneous anisotropic media with convex slowness surfaces were presented. The results for inhomogeneous media and more complicated anisotropy will be presented elsewhere. Although the considered models are relatively simple, several interesting phenomena were observed.

It seems that anisotropy has more pronounced effects on wave fields due to explosive sources than due to force sources. Explosive sources generate qS waves which may be of comparable intensity with correspondingly generated qP waves. Owing to the generation of only a single qS wave by an explosive source in a hexagonally symmetric medium, particle motion diagrams of direct waves in such media are linearly polarized (as in an isotropic medium). If the orientation of the

force source does not coincide with the axes of symmetry of the considered anisotropic medium, the nodal lines are shifted. Due to a general variation of the polarization vector with a variation of the slowness vector, the radiation pattern of the single force source may have more than two standard lobes.

The formulae presented in this paper are of importance not only in the study of radiation from point sources and in the construction of ray synthetic seismograms but also in other applications. For example, it would be possible to use the ray Green function (11) for the calculation of radiation from finite extent seismic sources (see e.g., ČERVENÝ *et al.*, 1987). The ray Green function (11) can also be used for the extension of the Born approximation algorithms from isotropic to anisotropic media. The above theory can also find important applications in the study of the effects of anisotropy on the AVO measurements. The importance of considering the effects of the source located in an anisotropic medium on the AVO results was pointed out recently, for example, by TSVANKIN (1995).

Acknowledgements

The authors are obliged to V. Červený and V. Vavryčuk for fruitful discussions and useful comments. Comments of reviewers are also acknowledged. Both authors appreciate the support of PPPG/UFBa, CNPq, PETROBRÁS and of the project Seismic waves in complex 3-D structures. Part of this study was undertaken during the stay of the first named author at the University of Hiroshima; the stay was organized by Kiyoshi Yomogida and supported by a JSPS Fellowship.

Appendix A. Calculation of the Geometrical Spreading

We define the geometrical spreading as the absolute value of the oriented cross section Ω of the ray tube and a phase front. The function Ω can be expressed as follows

$$\Omega = \left(\frac{\partial \vec{r}}{\partial \gamma_1} \times \frac{\partial \vec{r}}{\partial \gamma_2} \right)_\tau \cdot c\vec{p}. \tag{A.1}$$

Here γ_1 and γ_2 are the ray coordinates specifying a ray. We choose them as take-off angles φ_0 and δ_0 at the source so that the slowness vector $\vec{p}$ at the source has the form

$$\vec{p}(\tau_0) \equiv c_0^{-1}(\cos\varphi_0 \cos\delta_0, \sin\varphi_0 \cos\delta_0, \sin\delta_0). \tag{A.2}$$

The third ray coordinate γ_3 is chosen to be equal to the phase function τ. The ray

coordinates are chosen so that they form a right-handed coordinate system in isotropic media.

The function Ω is related to the Jacobian of the transformation from ray to Cartesian coordinates

$$\mathscr{T}_\tau = \begin{vmatrix} \left.\frac{\partial x_1}{\partial \gamma_1}\right|_\tau & \left.\frac{\partial x_1}{\partial \gamma_2}\right|_\tau & \frac{\partial x_1}{\partial \tau} \\ \left.\frac{\partial x_2}{\partial \gamma_1}\right|_\tau & \left.\frac{\partial x_2}{\partial \gamma_2}\right|_\tau & \frac{\partial x_2}{\partial \tau} \\ \left.\frac{\partial x_3}{\partial \gamma_1}\right|_\tau & \left.\frac{\partial x_3}{\partial \gamma_2}\right|_\tau & \frac{\partial x_3}{\partial \tau} \end{vmatrix} = \left(\frac{\partial \vec{r}}{\partial \gamma_1} \times \frac{\partial \vec{r}}{\partial \gamma_2}\right)_\tau \cdot \frac{d\vec{r}}{d\tau} = \Omega c \vec{p} \cdot \vec{v} = c\Omega.$$

Here v denotes the group velocity. To derive the formulae on the RHS we used eq. (A.1) and the identity

$$v_i p_i = 1. \tag{A.3}$$

To calculate the function Ω we need to evaluate the quantities $\partial x_k/\partial \gamma_J|_\tau$ and $\partial x_k/\partial \tau$. They can be obtained by solving the ray tracing and the dynamic ray tracing equations, see e.g. ČERVENÝ (1972), GAJEWSKI and PŠENČÍK (1990). If we write the ray tracing equations in the following form

$$\frac{dx_i}{d\tau} = \frac{1}{2}\frac{\partial G}{\partial p_i}, \quad \frac{dp_i}{d\tau} = -\frac{1}{2}\frac{\partial G}{\partial x_i},$$

the dynamic ray tracing has the form

$$\frac{dQ_{iJ}}{d\tau} = \frac{1}{2}\left[\frac{\partial^2 G}{\partial p_i \partial x_k} Q_{kJ} + \frac{\partial^2 G}{\partial p_i \partial p_k} P_{kJ}\right],$$

$$\frac{dP_{iJ}}{d\tau} = -\frac{1}{2}\left[\frac{\partial^2 G}{\partial x_i \partial x_k} Q_{kJ} + \frac{\partial^2 G}{\partial x_i \partial p_k} P_{kJ}\right],$$

where $Q_{kJ} = \partial x_k/\partial \gamma_J|_\tau$, $P_{kJ} = \partial p_k/\partial \gamma_J|_\tau$. The function $G(x_m, p_m)$ can be expressed as

$$G(x_m, p_m) = \rho^{-1} c_{ijkl} p_i p_l g_j g_k.$$

The equation

$$G(x_m, p_m) = 1$$

is the *eikonal equation* for inhomogeneous anisotropic media.

The dynamic ray tracing system consists of 12 linear ordinary differential equations. Their solution must satisfy four additional conditions so that only 8 of the 12 differential equations are independent. The first two conditions follow from the derivatives of the eikonal equation with respect to γ_1, γ_2, and read

$$\frac{\partial G}{\partial x_k} Q_{kJ} + \frac{\partial G}{\partial p_k} P_{kJ} = 0.$$

The other two conditions follow from the requirement that the slowness vector $\vec{p}$ be perpendicular to the phase front and thus $\vec{p}$ is also perpendicular to any vector tangent to the phase front. Since the vectors $Q_{kJ} = \partial x_k / \partial \gamma_J|_\tau$ for $J = 1, 2$ are tangent to the phase front, we have

$$p_k Q_{kJ} = 0.$$

In order to solve the ray tracing and dynamic ray tracing equations, it is necessary to specify appropriate initial conditions for x_i and p_i, and Q_{iJ} and P_{iJ}. For a point source situated in an inhomogeneous anisotropic medium and for the slowness vector specified by the above introduced ray parameters $\gamma_1 = \varphi_0$ and $\gamma_2 = \delta_0$, see (A.2), the initial conditions for the ray tracing equations have the form

$$x_i(\tau_0) = 0, \quad p_i(\tau_0) = c_0^{-1} N_i^0,$$

where

$$N_1^0 = \cos\varphi_0 \cos\delta_0, \quad N_2^0 = \sin\varphi_0 \cos\delta_0, \quad N_3^0 = \sin\delta_0.$$

The initial conditions for the dynamic ray tracing equations are:

$$Q_{iJ}(\tau_0) = 0, \quad P_{iJ}(\tau_0) = c_0^{-1}\left(\frac{\partial N_i^0}{\partial \gamma_J} - p_i^0 v_k(\tau_0) \frac{\partial N_k^0}{\partial \gamma_J}\right), \tag{A.4}$$

where

$$\frac{\partial N_1^0}{\partial \varphi_0} = -\sin\varphi_0 \cos\delta_0, \quad \frac{\partial N_2^0}{\partial \varphi_0} = \cos\varphi_0 \cos\delta_0, \quad \frac{\partial N_3^0}{\partial \varphi_0} = 0,$$

$$\frac{\partial N_1^0}{\partial \delta_0} = -\cos\varphi_0 \sin\delta_0, \quad \frac{\partial N_2^0}{\partial \delta_0} = -\sin\varphi_0 \sin\delta_0, \quad \frac{\partial N_3^0}{\partial \delta_0} = \cos\delta_0.$$

In a homogeneous anisotropic medium, the dynamic ray tracing specified by the above initial conditions yields the function Ω in the following form

$$\Omega = r^2 K \frac{v^2}{c^4} |\cos\delta_0|,$$

see Appendix B. Here K denotes the Gaussian curvature of the slowness surface.

By inspecting eq. (4) we can see that the ray amplitudes are proportional to quantity $(\Omega(x_{om})/\Omega(x_m))^{1/2}$. This means that for the angle δ_0 approaching $\pi/2$, the dynamic ray tracing with the initial conditions (A.4) leads to complications in the calculation of amplitudes. The amplitudes are specified by formulae in which the nominator and the denominator approach zero in the same way. As pointed out by ČERVENÝ (1985) this is an unnecessary complication. It can be avoided if we specify the initial conditions for the dynamic ray tracing system as follows

$$Q_{iJ}(\tau_0) = 0, \quad P_{iJ}(\tau_0) = R_{iJ} - p_i^0 v_k(\tau_0) R_{kJ}, \tag{A.5}$$

where

$$R_{11} = -\sin\varphi_0, \quad R_{21} = \cos\varphi_0, \quad R_{31} = 0,$$

$$R_{12} = -\cos\varphi_0 \sin\delta_0, \quad R_{22} = -\sin\varphi_0 \sin\delta_0, \quad R_{32} = \cos\delta_0.$$

The initial conditions (A.4) are a special case of (A.5). They can be obtained from (A.5) by multiplying the vector $P_{i1}(\tau_0)$ by the constant factor $c_0^{-1}\cos\delta_0$ and the vector $P_{i2}(\tau_0)$ by the constant factor c_0^{-1}. Since the dynamic ray tracing is linear, its solution with the initial conditions (A.4) can be obtained from the solution with the initial conditions (A.5) by the multiplication by the same constant factors. In this way the initial conditions (A.5) yield a function Ω_M different from Ω specified by (A.4). The function Ω_M for a homogeneous anisotropic medium attains the form

$$\Omega_M = (v/c)^2 K r^2,$$

see Appendix B. In a similar way as in KENDALL *et al.* (1992), it is possible to show that the function Ω_M obtained from the dynamic ray tracing specified by the initial conditions (A.5) is reciprocal. We adopt here the terminology used by ČERVENÝ (1995) for the reciprocal geometrical spreading in an isotropic medium and call $|\Omega_M|$ the *relative geometrical spreading*.

Appendix B. Relation of the Function Ω and the Curvature of the Slowness Surface K in a Homogeneous Medium

Equation (A.1) can be rewritten as follows

$$\Omega c\vec{p} = \left(\frac{\partial\vec{r}}{\partial\gamma_1} \times \frac{\partial\vec{r}}{\partial\gamma_2}\right)_\tau.$$

In the next the index τ is omitted. Let us multiply the above equation by the group velocity vector $\vec{v}$ expressed in the following way

$$\vec{v} = v\,\frac{\dfrac{\partial\vec{p}}{\partial\gamma_1} \times \dfrac{\partial\vec{p}}{\partial\gamma_2}}{\left|\dfrac{\partial\vec{p}}{\partial\gamma_1} \times \dfrac{\partial\vec{p}}{\partial\gamma_2}\right|}.$$

We took into account that the group velocity vector is perpendicular to the slowness surface. From the resulting equation, considering the equation (A.3), we get

$$\Omega = \frac{v}{c}\,\frac{\left(\dfrac{\partial\vec{r}}{\partial\gamma_1}\cdot\dfrac{\partial\vec{p}}{\partial\gamma_1}\right)\left(\dfrac{\partial\vec{r}}{\partial\gamma_2}\cdot\dfrac{\partial\vec{p}}{\partial\gamma_2}\right) - \left(\dfrac{\partial\vec{r}}{\partial\gamma_1}\cdot\dfrac{\partial\vec{p}}{\partial\gamma_2}\right)\left(\dfrac{\partial\vec{r}}{\partial\gamma_2}\cdot\dfrac{\partial\vec{p}}{\partial\gamma_1}\right)}{\left|\dfrac{\partial\vec{p}}{\partial\gamma_1} \times \dfrac{\partial\vec{p}}{\partial\gamma_2}\right|}.$$

From the ray tracing equations $d\vec{r}/d\tau = \vec{v}$ specified for a homogeneous medium, we have

$$\frac{\partial \vec{r}}{\partial \gamma_I} = \frac{\partial \vec{v}}{\partial \gamma_I} \frac{r}{v}.$$

Using this relation we can write

$$\frac{\partial \vec{r}}{\partial \gamma_I} \cdot \frac{\partial \vec{p}}{\partial \gamma_J} = \frac{r}{v} \frac{\partial \vec{v}}{\partial \gamma_I} \cdot \frac{\partial \vec{p}}{\partial \gamma_J} = \frac{r}{v} \frac{\partial}{\partial \gamma_I} \left(\vec{v} \cdot \frac{\partial \vec{p}}{\partial \gamma_J} \right) - \frac{r}{v} \vec{v} \cdot \frac{\partial^2 \vec{p}}{\partial \gamma_I \partial \gamma_J}.$$

The term in the brackets is zero because of the perpendicularity of the group velocity vector to the slowness surface and thus

$$\frac{\partial \vec{r}}{\partial \gamma_I} \cdot \frac{\partial \vec{p}}{\partial \gamma_J} = -\frac{r}{v} \vec{v} \cdot \frac{\partial^2 \vec{p}}{\partial \gamma_I \partial \gamma_J}. \tag{B.1}$$

The formula for the function Ω can now be rewritten into the form

$$\Omega = \frac{r^2}{vc} \frac{\left(\vec{v} \cdot \frac{\partial^2 \vec{p}}{\partial \gamma_1^2} \right) \left(\vec{v} \cdot \frac{\partial^2 \vec{p}}{\partial \gamma_2^2} \right) - \left(\vec{v} \cdot \frac{\partial^2 \vec{p}}{\partial \gamma_1 \partial \gamma_2} \right)^2}{\left| \frac{\partial \vec{p}}{\partial \gamma_1} \times \frac{\partial \vec{p}}{\partial \gamma_2} \right|} = \frac{r^2}{vc} K v^2 \left| \frac{\partial \vec{p}}{\partial \gamma_1} \times \frac{\partial \vec{p}}{\partial \gamma_2} \right|.$$

Here K is the Gaussian curvature of the slowness surface. For the formula for the Gaussian curvature of a surface see, e.g., KORN and KORN (1961). It is easy to show that for the initial conditions of the dynamic ray tracing equations (A.4) the following identity holds

$$\left| \frac{\partial \vec{p}}{\partial \gamma_1} \times \frac{\partial \vec{p}}{\partial \gamma_2} \right| = \frac{v}{c^3} |\cos \delta_0|$$

and thus for the initial conditions (A.4) the function Ω in a homogeneous anisotropic medium has the form

$$\Omega = r^2 K \left(\frac{v}{c^2} \right)^2 |\cos \delta_0|.$$

For the initial conditions (A.5), we get

$$\Omega_M = r^2 K \left(\frac{v}{c} \right)^2. \tag{B.2}$$

In homogeneous isotropic media, eq. (B.2) reduces to

$$\Omega_M = r^2 c^2. \tag{B.3}$$

Appendix C. Specification of the Index of the Source

Here we demonstrate the use of the quantities calculated in the dynamic ray tracing for the determination of the index of the source. For this purpose we express the principal curvatures of the slowness surface at the source in terms of $\partial\vec{r}/\partial\gamma_I$ and $\partial\vec{p}/\partial\gamma_I$. The principal curvatures k are solutions of the quadratic equation

$$(L-kE)(N-kG)-(M-kF)^2=0, \tag{C.1}$$

where

$$L=v^{-1}\left(\vec{v}\cdot\frac{\partial^2\vec{p}}{\partial\gamma_1^2}\right), \quad M=v^{-1}\left(\vec{v}\cdot\frac{\partial^2\vec{p}}{\partial\gamma_1\gamma_2}\right), \quad N=v^{-1}\left(\vec{v}\cdot\frac{\partial^2\vec{p}}{\partial\gamma_2^2}\right),$$

$$E=\left(\frac{\partial\vec{p}}{\partial\gamma_1}\cdot\frac{\partial\vec{p}}{\partial\gamma_1}\right), \quad F=\left(\frac{\partial\vec{p}}{\partial\gamma_1}\cdot\frac{\partial\vec{p}}{\partial\gamma_2}\right), \quad G=\left(\frac{\partial\vec{p}}{\partial\gamma_2}\cdot\frac{\partial\vec{p}}{\partial\gamma_2}\right).$$

We can use relation (B.1) and express L, M and N in terms of the quantities which are solutions of the dynamic ray tracing:

$$L=-r^{-1}\left(\frac{\partial\vec{r}}{\partial\gamma_1}\cdot\frac{\partial\vec{p}}{\partial\gamma_1}\right), \quad M=-r^{-1}\left(\frac{\partial\vec{r}}{\partial\gamma_1}\cdot\frac{\partial\vec{p}}{\partial\gamma_2}\right), \quad N=-r^{-1}\left(\frac{\partial\vec{r}}{\partial\gamma_2}\cdot\frac{\partial\vec{p}}{\partial\gamma_2}\right).$$

Using the solution of eq. (C.1) in (8), we gain alternative rules for the determination of the index of the source:

$$k_S=0 \quad \text{if} \quad a>0 \quad \text{and} \quad b<0,$$

$$k_S=1 \quad \text{if} \quad a<0,$$

$$k_S=2 \quad \text{if} \quad a>0 \quad \text{and} \quad b>0,$$

where

$$a=EG-F^2, \quad b=LG+NE-2MF.$$

The quantity a is proportional to the product and b to the sum of the principal curvatures.

References

AKI, K., and RICHARDS, P. G., *Quantitative Seismology* (W. H. Freeman, San Francisco 1980).

BEN-MENAHEM, A., GIBSON, R., JR., and SENA, A. (1991), *Green's Tensor and Radiation Patterns of Point Sources in General Anisotropic Inhomogeneous Elastic Media*, Geophys. J. Int. *107*, 297–308.

BLEISTEIN, N., *Mathematical Methods for Wave Phenomena* (Academic Press, London 1984).

BUCHWALD, V. (1959), *Elastic Waves in Anisotropic Media*, Proc. R. Soc. London *235*, 563–580.

BURRIDGE, R. (1967), *The Singularity on the Plane Lids of the Wave Surface of Elastic Media with Cubic Symmetry*, Q. J. Mech. Appl. Math. *20*, 41–56.

ČERVENÝ, V. (1972), *Seismic Rays and Intensities in Inhomogeneous Anisotropic Media*, Geophys. J. R. Astr. Soc. *29*, 1–13.

ČERVENÝ, V., *The application of ray tracing to the numerical modeling of seismic wave field in complex structures*. In *Handbook of Geophysical Exploration, Section 1: Seismic Exploration* (eds. Helbig, K. and Treitel, S.) *Seismic Shear Waves* (ed. Dohr, G.) (Geophysical Press, London 1985) pp. 1–124.

ČERVENÝ, V., *Seismic Waves in Anisotropic Media. Lecture Notes* (Petrobrás, Rio de Janeiro 1990).

ČERVENÝ, V., *Seismic Wave Fields in Three-dimensional Isotropic and Anisotropic Structures, Lecture Notes* (University of Trondheim 1995).

ČERVENÝ, V., MOLOTKOV, I. A., and PŠENČÍK, I., *Ray Method in Seismology* (Universita Karlova, Praha 1977).

ČERVENÝ, V., PLEINEROVÁ, J., KLIMEŠ, L., and PŠENČÍK, I. (1987), *High-frequency Radiation from Earthquake Sources in Laterally Varying Layered Structures*, Geophys. J. R. Astr. Soc. *88*, 43–79.

GAJEWSKI, D. (1993), *Radiation from Point Sources in General Anisotropic Media*, Geophys. J. Int. *113*, 299–317.

GAJEWSKI, D., and PŠENČÍK, I. (1990), *Vertical Seismic Profile Synthetics by Dynamic Ray Tracing in Laterally Varying Layered Anisotropic Structures*, J. Geophys. Res. *95*, 11301–11315.

HANYGA, A. (1984), *Point Source in Anisotropic Medium*, Gerlands Beitr. Geophys. *93*, 463–479.

HUDSON, J. A. (1981), *Wave Speeds and Attenuation of Elastic Waves in Materials Containing Cracks*, Geophys. J. R. Astr. Soc. *64*, 487–497.

KAWASAKI, I., and TANIMOTO, T. (1981), *Radiation Patterns of Body Waves due to the Seismic Dislocation Occurring in an Anisotropic Source Medium*, Bull. Seismol. Soc. Am. *71*, 37–50.

KENDALL, J.-M., GUEST, W., and THOMSON, C. (1992), *Ray-theory Green's Function Reciprocity and Ray-centered Coordinates in Anisotropic Media*, Geophys. J. Int. *108*, 364–371.

KORN, G. A., and KORN, T. M., *Mathematical Handbook for Scientists and Engineers* (McGraw-Hill, New York 1961).

KOSEVICH, A. M., and NATSIK, V. D. (1964), *Elastic Field of Continuously Distributed Moving Dislocation Loops*, Soviet Phys. Solid State *6*, 181–186.

KUMAZAWA, M., and ANDERSON, O. L. (1969), *Elastic Moduli, Pressure Derivatives and Temperature Derivatives of Single Crystal Olivine and Single Crystal Fosterite*, J. Geophys. Res. *74*, 5961–5972.

SHEARER, P. M., and CHAPMAN, C. H. (1989), *Ray Tracing in Azimuthally Anisotropic Media—I. Results of Modes of Aligned Cracks in the Upper Crust*, Geophys. J. Int. *96*, 51–64.

TELES, N. T. (1995), *Study of Effects of Seismic Sources Situated in Anisotropic Media on Ray Synthetic Seismograms*, Ph.D. Thesis, Universidade Federal da Bahia (in Portuguese).

TSVANKIN, I. (1995), *Body-wave Radiation Patterns and AVO in Transversely Isotropic Media*, Geophysics *60*, 1409–1425.

TSVANKIN, I., and CHESNOKOV, E. (1990a), *Synthesis of Body Wave Seismograms from Point Sources in Anisotropic Media*, J. Geophys. Res. *95*, 11,317–11,331.

TSVANKIN, I., and CHESNOKOV, E. (1990b), *Synthetic Waveforms and Polarizations at the Free Surface of an Anisotropic Half-space*, Geophys. J. Int. *101*, 497–505.

YEATTS, F. (1984), *Elastic Radiation from a Point Source in an Anisotropic Medium*, Phys. Rev. B. Condens. Matter. *29*, 1674–1684.

(Received July 17, 1995, revised December 21, 1995, accepted January 22, 1996).